FEMS Microbiology Ecology, 92, 2016, fiw053

doi: 10.1093/femsec/fiw053
Advance Access Publication Date: 13 March 2016
Research Article

RESEARCH ARTICLE

Evidence for marine origin and microbial-viral habitability of sub-zero hypersaline aqueous inclusions within permafrost near Barrow, Alaska

J. Colangelo-Lillis[1,*], H. Eicken[2], S. D. Carpenter[1] and J. W. Deming[1]

[1]School of Oceanography and Astrobiology Program, University of Washington, Seattle, WA, 98195, USA and [2]International Arctic Research Center, University of Alaska Fairbanks, Fairbanks, AK, 99775, USA

*Corresponding author: Department of Earth and Planetary Science, McGill University, 3450 University Street, Montreal, Quebec, H3A 0E8, Canada. Tel: (514)-398-6767; Fax: 514.398.4680; E-mail: jesse.colangelo-lillis@mail.mcgill.ca

One sentence summary: Measurements made from liquid brine within Arctic permafrost indicate an ancient marine origin, active viral–microbe dynamics and large amounts of extracellular polysaccharide substances.

Editor: Dirk Wagner

ABSTRACT

Cryopegs are sub-surface hypersaline brines at sub-zero temperatures within permafrost; their global extent and distribution are unknown. The permafrost barrier to surface and groundwater advection maintains these brines as semi-isolated systems over geological time. A cryopeg 7 m below ground near Barrow, Alaska, was sampled for geochemical and microbiological analysis. Sub-surface brines (*in situ* temperature of –6 °C, salinity of 115 ppt), and an associated sediment-infused ice wedge (melt salinity of 0.04 ppt) were sampled using sterile technique. Major ionic concentrations in the brine corresponded more closely to other (Siberian) cryopegs than to Standard seawater or the ice wedge. Ionic ratios and stable isotope analysis of water conformed to a marine or brackish origin with subsequent Rayleigh fractionation. The brine contained ∼1000× more bacteria than surrounding ice, relatively high viral numbers suggestive of infection and reproduction, and an unusually high ratio of particulate to dissolved extracellular polysaccharide substances. A viral metagenome indicated a high frequency of temperate viruses and limited viral diversity compared to surface environments, with closest similarity to low water activity environments. Interpretations of the results underscore the isolation of these underexplored microbial ecosystems from past and present oceans.

Keywords: sub-surface microbiology; oxygen isotopes; hydrogen isotopes

INTRODUCTION

Cryopegs are brine lenses within permafrost, and their liquid state is maintained at sub-zero temperatures by high concentrations of solutes. Reports on the existence of cryopegs are sparse. While their discovery has been serendipitous, ground penetrating radar suggests that they are a common feature of permafrost systems, often found immediately above the permafrost base (Tolstikhin and Tolstikhin 1974; van Everdingen 1976). Only three such systems, all in Eastern Siberia, have been characterized for their microbial constituents (Gilichinsky *et al.* 2003; Pecheritsyna *et al.* 2007; Fig. 1). The Lake Yakutskoye and Kolymskaya cryopegs were found at depths of 8–28 m below ground surface and were 0.5–1.5 m thick and 3–5 m wide (Gilichinsky *et al.* 2003); the Varandei Peninsula cryopegs were identified from shallow boreholes ≤9 m below ground surface (their extent was not reported; Pecheritsyna *et al.* 2007). All of these sites are located within close proximity (<5 km) of the continental coast.

Received: 12 November 2015; **Accepted:** 5 March 2016

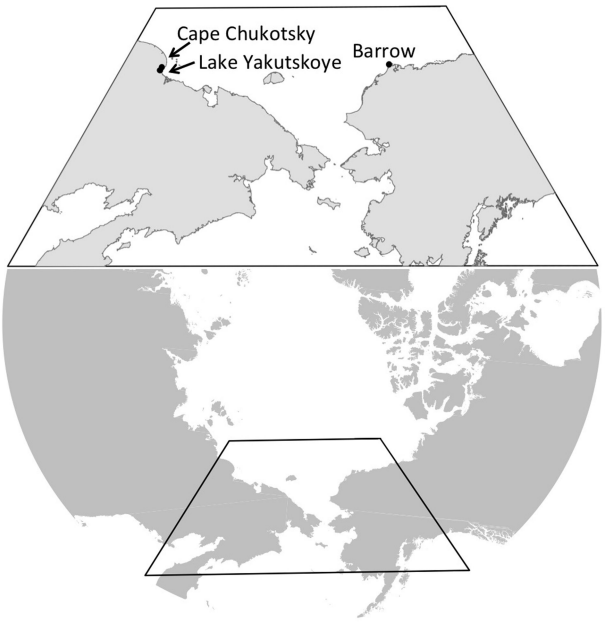

Figure 1. Location of Siberian cryopegs that have been investigated as microbial habitats and the Alaskan cryopeg of this study.

Based on local geology and aqueous chemistry, the formation of previously described Siberian cryopegs was attributed to the concentration of marine sediment pore waters after sub-aerial exposure and freezing in response to sea level drop ~100 Ka ago; terrigenous deposition followed (at ~26 Ka), and the freezing of this material isolated the concentrated marine brines from the atmosphere and meteoric water (Gilichinsky *et al.* 2003). Geochemical analyses demonstrated that the brines were anoxic, with elevated salinities of 170–300 g L^{-1}, circumneutral pH and ion concentrations exceeding modern seawater concentrations twofold (K^+, SO_4^{2-}) to 5-fold (Cl^-, Ca^{2+}, Mg^{2+}, Na^+; Gilichinsky *et al.* 2003; Pecheritsyna *et al.* 2007).

Pioneering work on the microbiology of Siberian cryopegs led to culture-based identification of numerous microbial metabolisms including aerobic and anaerobic heterotrophs, sulfate reducers, acetogens and methanogens (Gilichinsky et al. 2003, 2005); community activity based on uptake of ^{14}C-glucose in samples incubated at –15 °C (Gilichinsky *et al.* 2003); and isolation and characterization of new psychrophilic species of *Clostridium* and *Psychrobacter,* and new psychrotolerant species of *Desulfovibrio* (Shcherbakova et al., 2004, 2005, 2009; Pecheritsyna et al. 2007, 2012) and of nitrogen-fixing *Celerinatantimonas* (Shcherbakova *et al.* 2013). Due to extremes of temperature and salinity, and confinement from surface processes, these brines have been considered analog environments for contemporary or transient extraterrestrial microbial habitats, particularly on Mars (Gilichinsky *et al.* 2003). The total density of bacteria inhabiting Siberian cryopegs has been reported rarely; in one case, propidium iodide staining yielded 10^7 microorganisms ml^{-1} (Gilichinsky *et al.* 2005), a value that exceeds densities typically observed in seawater by an order of magnitude but falls in the range of those observed in the brines of sea ice (Deming 2010; Boetius *et al.* 2015). A defining characteristic of sea-ice brine is its elevated content of extracellular polysaccharide substances (EPS; Krembs, Eicken and Deming 2011), which serve numerous functions for the microbial inhabitants, including cyroprotection, osmoprotection and possibly viral defense (Marx, Carpenter and Deming 2009; Colangelo-Lillis and Deming 2013). The presence of EPS in cryopegs has not been examined.

Numerous other hypersaline aqueous microbial habitats have been geochemically and microbiologically characterized, including some outside of the cryosphere, such as hypersaline lakes (Ward *et al.* 2000), salterns and crystallizer ponds (Antón *et al.* 2000), as well as cold sites (here defined as <4 °C; Deming 2010), including deep ocean brine pools (van der Wielen *et al.* 2005), polar hypersaline lakes and springs (Siegel *et al.* 1979; Rankin *et al.* 1996; Perreault *et al.* 2007) and the brines of sea ice (Deming 2010; Thomas, Papadimitriou and Michel 2010). These environments are categorized as thalassohaline or athalassohaline based on their genesis and resultant ionic composition: thalassohaline are of marine origin, athalassohaline originate from freshwater sources. Despite the widespread occurrence of these hypersaline aqueous systems across latitudes, their dissimilarity from cryopegs stems from their rate of interaction with atmosphere, ground water, light and surface processes. A notable hypersaline ecosystem with some degree of isolation from these influences, making it more comparable to cryopegs, is Lake Vida of the Antarctic Dry Valleys. Athalassohaline Lake Vida is frozen throughout the year, with an ice cover tens of meters thick, while maintaining a network of brines at –13.5 °C and 6-fold seawater salinity. The lake houses a diverse community of microorganisms thought to be supported by free energy-releasing redox couples associated with interactions between brine and iron-rich sediment (Murray *et al.* 2012). Qualitative microscopic observations suggest that EPS may play a role in the activities of some of these microorganisms (Murray *et al.* 2012). Lake Vida brine is anoxic, and water recovered from the lake turns from light yellow to dark orange upon exposure to the atmosphere as a result of ferric iron oxidation and precipitation. Based on carbon dating of organic material preserved in the overlying ice, the system is thought to have been isolated on the scale of thousands of years. Exhibiting even longer isolation from the atmosphere are the brines below Taylor Glacier, the source of Blood Falls in the Dry Valleys of Antarctica. These brines appear to house marine-derived sulfur-metabolizing communities that have been isolated for over a million years (Mikucki *et al.* 2009). The microbial communities of both Lake Vida and Blood Falls differ from Siberian cryopegs in their considerably lower abundances: $1-6 \times 10^5$ DAPI-stained microorganisms ml^{-1} in Lake Vida (Murray *et al.* 2012) and 6×10^4 ml^{-1} in Blood Falls (Mikucki *et al.* 2009). Due to their isolation and the logistical hurdles to exploration and experimentation, few of the processes that drive microbial ecology have been explored in these systems.

The impact of viruses on marine microbial communities has received considerable attention, from their abundance and genetic diversity to their roles in controlling microbial populations and mediating lateral gene transfer (Rohwer and Thurber 2009). While viruses have been found in every habitat investigated for their presence, including sub-zero hypersaline environments (Deming 2010), their role in such extreme environments are less well explored. High concentrations of viruses have been reported for both warm and cold hypersaline ecosystems (Rodriguez-Brito *et al.* 2010; Collins and Deming 2011; Santos *et al.* 2012), with the highest densities reported from salterns (>10^{10} ml^{-1}; Santos *et al.* 2012) and winter sea-ice brines (>10^9 ml^{-1}; Collins and Deming 2011). Evidence of viral production and microbial growth has been obtained at the low temperatures (down to −12 °C) and high salinities (up to 160 ppt) found in such brines (Wells and Deming 2006c). Whether these high viral concentrations reflect slower decay rates (as shown under winter sea-ice brine conditions; Wells and Deming 2006c), greater

burst sizes, or a high incidence of non-lethal viral replication (e.g. chronic infection) remain open questions. High concentrations of virus-sized particles (<200 nm) have been detected in Lake Vida, though full attribution to viruses is uncertain and viral diversity and activity remain unexplored (Murray *et al.* 2012). The presence of viruses in other Antarctic lakes, with seasonal or no ice cover, has been reported (DeMaere *et al.* 2013); in exceptional cases, elements of viral infection dynamics have been described (Laybourn-Parry, Marshall and Madan 2007; Yau *et al.* 2011). In each case, the study of viruses from these environments has expanded our understanding of viral diversity in form and ecological impact; the viral content of cryopeg brines has not been reported.

Sub-terranean, ice-associated microbial habitats are difficult environments to study. Interactions between rock and brine and their role in providing energy to, or selection pressures on, the microbes within remain underexplored. Investigating these environments and processes is relevant to understanding the global diversity of microbial metabolisms, the persistence of communities in the absence of photoautotrophy, including potential metabolic synergies between organisms utilizing the metabolic output of a neighbor, and the search for biosignatures in extreme or extraterrestrial environments. In this initial study of a cryopeg near Barrow, Alaska, we sought through opportunistic sampling to expand knowledge of cryopegs beyond the Siberian systems by evaluating the origin and microbial habitability of this Alaskan cryopeg, including EPS content, the viral community and potential activity in this cold, dark and hypersaline environment.

MATERIALS AND METHODS

Site description

The cryopeg system sampled was accessed via the Barrow Permafrost Tunnel (coordinates: 71.2944 °N, 156.7153 °W; Fig. 1), which was excavated in the 1960s by the US Army Cold Regions Research and Engineering Laboratory (CRREL; Brown 1965). The tunnel's vertical access shaft descends 6 m through two intersecting ice wedges to reach a horizontal excavation, running East–West that is 2 m high, 1.5 m wide and 10 m long (Fig. 2; Fig. S1 a—c, Supporting Information). Cryopeg brines, initially detected in 2004 reside ~1.3 m below its floor (Yoshikawa *et al.* 2004). The surrounding ice wedges, indicative of sustained subfreezing temperatures since formation, have been carbon-dated to 14 Ka ago (Meyer *et al.* 2010), suggesting a potential minimum age for the cryopeg brines. This is the first description of the character of these or any other cryopeg brines outside of Siberia, though the surrounding ice wedges, including isotopic composition of water and entrained organic carbon, have been described (Meyer *et al.* 2010).

Sampling

Cryopeg brines were collected from below the floor of the permafrost tunnel over a period of six days in August 2009. Brines were recovered by hand pump, using sterilized tubing and vacuum flasks, through two 2 cm wide polyvinylchloride pipes extending from the tunnel floor into the brine below (Fig. 2). One of these pipes (see CB1 in Fig. 2 and image (d) in Fig. S1, Supporting Information) had been installed previously and was uncapped for sampling purposes; the second pipe was installed on the fourth day of sampling into a pre-existing hole (see CB3 in Fig. 2) that contained ice to 5 cm below the floor of the tunnel upon initial investigation. A third hole was drilled to 1.5 m using an ice auger (see IA in Fig. 2) during this sampling campaign to evaluate spatial distribution of the brine. Sterile techniques and materials (e.g. ethanol washing of fiber glass corer barrel and brass/steel corer head) were used to the greatest extent possible in the process. Brine temperature and pH were measured at the time of collection with a handheld infrared temperature probe and pH paper. Brines were transferred to sterile polypropylene bottles and transported in temperature-equilibrated, insulated coolers, within 15 min, to the Barrow Arctic Research Center (BARC) laboratory. Sub-samples of cryopeg brine were fixed to final concentration of 2% formaldehyde for bacterial and viral counts. Brine samples were kept at –1 °C for transport to Seattle, WA.

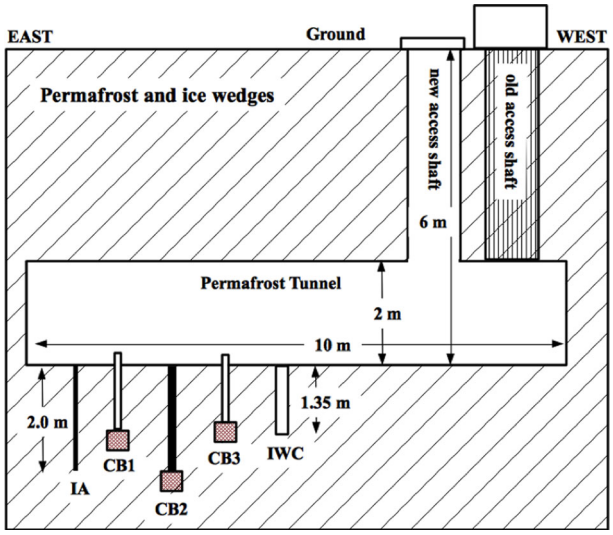

Figure 2. Schematic of the Barrow Permafrost Tunnel and access to the cryopeg brine reservoir. The tunnel was entered through the new access shaft (the old one was filled with debris). Three cryopeg brine holes already existed: CB1, a capped PVC pipe, 2 cm wide, 1.3 m deep, sampled for brine; CB2, 10 cm wide, depth unknown, filled with orange-colored ice, not sampled; and CB3, partially ice-filled, newly fitted with PVC pipe 2 cm wide, 1.0 m deep, sampled for brine. New IA hole was 5 cm wide, 2 m deep and yielded no brine. Ice wedge core (IWC) hole was 12 cm diameter, 1.3 m depth. Cross-hatched boxes at base of CB1-3 represent pools of cryopeg brine, not drawn to scale.

On the fifth of six sampling days, a single ice wedge core, 135 cm long, was collected using an 8.5 cm inner diameter CRREL-style core barrel; temperature at the base of the core was measured upon collection (Fig. S1c, Supporting Information). The core was transported within the core barrel to the BARC cold room (–10 °C), where it was removed (Fig. S1h, Supporting Information) and cut into thirteen 10 cm and one 5 cm sections using an ethanol-sterilized handsaw. These sections were placed into sterile plastic sleeves and transported frozen to Seattle, WA. Sub-samples for further analyses were melted in a 2 °C cold laboratory. As for brine samples, melted ice sub-samples were fixed in formaldehyde to determine bacterial and viral abundance. Unfixed samples were processed for other analyses.

Salinity and major ions

Salinity of the brine and melted ice core sections was determined from conductivity measurements using a handheld YSI-30 conductivity meter. Geochemical analysis of major ions was completed at the Cold Regions Research and Engineering Laboratory (CRREL) Alaska Geochemistry Laboratory, using methods described by Douglas *et al.* (2012). Cation and anion concentrations of filtered samples of brine (diluted by three orders of

magnitude) and melted ice from each individual core section were determined with a Dionex ICS-3000 ion chromatograph with an AS-19 anion column and CS-12 cation column (Dionex Corporation Sunnyvale, California). Details on injection volumes, flow rates and use of eluents are provided by Douglas *et al.* (2012). Calibration with anion and cation laboratory standards in repeat analysis resulted in a calculated precision of 5% for the measurements. Peaks were identified using Chromeleon software (Dionex, Sunnyvale, California) and were verified visually.

Stable isotopes

Stable isotope measurements of the brine and ice core samples were made at the Alaska Stable Isotope Facility of the Water and Environmental Research Center, University of Alaska Fairbanks. A thermal conversion elemental analyzer (TC/EA) attached via a Conflo III to a Thermo delta XP isotope ratio mass spectrometer (IRMS) was used to measure δD and δ^{18}O values of samples against Vienna Standard Mean Ocean Water (VSMOW) at a precision better than 1.5 ‰ (δD) and 0.2 ‰ (δ^{18}O). To evaluate deviations from atmospheric Rayleigh fractionation, deuterium excess (DE) was calculated as $DE = \delta^2H - 8 \cdot \delta^{18}O$, following Dansgaard (1964). Triplicate measurements were made from each section of the ice core and (separately) on brine recovered from CB1 and CB3 (Fig. 2).

Particulate measurements

The concentration of suspended particulate matter (SPM) was determined following filtration of known sample volumes through 42.5 mm, pre-combusted, pre-weighed GF/C filters. Filters were rinsed with 10 ml of 1% sodium formate to remove salts, dried at 60 °C for 24 h and reweighed to calculate the total dry weight of SPM (Williams 1985). Single measurements were made from each section of the ice core. Concentrations of particulate organic carbon (POC) and particulate nitrogen (PN) were quantified using a Leeman Labs Model CEC440 Elemental Analyzer after removing inorganic carbon from the pre-combusted filters by fuming with HCl (as in Kellogg and Deming 2009). Particulate (>0.4 μm) and dissolved (<0.4 μm) extracellular polysaccharide substances (pEPS and dEPS, respectively) were measured using the phenol sulfuric acid method of Dubois *et al.* (1956), following Ewert *et al.* (2013) without their dialysis step. Results were quantified as glucose equivalents (glucose was used to generate the standard curve against which measurements were calibrated), and converted to carbon using a conversion factor of 0.75 (following Engel and Passow 2001, as in Krembs *et al.* 2002). Duplicate measurements of POC, PN and pEPS and dEPS were made for each section of the ice core, and separately for brine recovered from CB1 and from CB3 (Fig. 2).

Bacterial and viral abundance

The abundance of total bacteria (here used to indicate members of the domains Bacteria and Archaea) and virus-like particles (VLP) for both cryopeg brines and melted ice sections were determined by epifluorescence microscopy on the formaldehyde-fixed samples. For bacteria, samples were filtered through 0.2 μm pore-size, black polycarbonate filters and stained with DAPI, following Ewert *et al.* (2013). For viral enumeration, samples were filtered through 0.02 μm pore-size anodiscs and stained with SYBR Green I, following Noble and Fuhrmann (1998). Individual slides were prepared for bacterial enumeration from each section of the ice core and duplicates were prepared for brines from CB1 and CB3 (Fig 2.). Due to a manufacturing cessation on 0.02 μm pore-size anodisc filters, ice core VLP concentration was determined from duplicate VLP slides prepared from a single section (100–110 cm depth below permafrost tunnel). Duplicate VLP slides were prepared for brines from CB1 and CB3. To confirm identity of fluorescing VLP as viruses, these particles were adsorbed to carbon-stabilized, formvar-coated copper grids, uranyl acetate stained and examined using a PJEOL JEM 1200EXII (Ted Pella Inc., Redding, CA, USA) transmission electron microscope at 100 kV acceleration voltage.

Viral metagenome

The viral fraction for metagenomic analysis was collected by 0.2 μm filtration of 500 ml of cryopeg brine from CB1 (Fig. 2), and stored at –4°C until further processing. The filtrate was first purified by polyethylene glycol precipitation (10% wt/vol, centrifugation 13 000 *g*, 60 min), then incubated with chloroform to disrupt any residual cells (0.7X vol, 15 min), followed by DNase I to degrade free DNA (120 min, 37°C). Viral DNA was extracted using a MinElute Virus Spin Kit (QIAGEN cat. 57704). Extracted DNA was sheared, primer ligated (Duhaime *et al.* 2012) and sent to the Broad Institute for 454 Titanium pyrosequencing (454 Life Sciences, Branford, CT) as part of the Gordon and Betty Moore Marine Microbiology Initiative (Henn *et al.* 2010). Bioinformatic analyses were performed with software tools provided by MG-RAST (Meyer *et al.* 2008) and MetaVir (Roux *et al.* 2011). Sequence data are deposited at NCBI Genbank under SRA no. SRX042535.

RESULTS

On site observations

The temperature of ambient air within the permafrost tunnel was recorded as –3.8 °C; the floor of the tunnel was –5.0 °C. The cryopeg brines and the bottom of the ice core (135 cm below the tunnel floor) were recorded as –6.0 °C. Cryopeg brine from CB1 (Fig 2.) was nearly colorless upon extraction, but acquired a degree of orange coloration shortly after collection, which intensified with storage (Fig. S1g, Supporting Information). Brine from CB3 was darker, and brown in color, apparently as a result of higher sediment load; no change in color was observed following its collection. Consolidated ices inside pre-existing holes CB2 and CB3 (Fig. 2) were also orange in color (Fig. S1d and e, Supporting Information), as were several small patches (<100 cm^2) of hoar-frost ice observed on the ceiling of the tunnel approximately above the sampling pipe for CB1 (Fig. 2; Fig. S1f, Supporting Information). The extent of these orange ice crystals did not change over our sampling period. Brine volumes collected from the existing pipe (accessing CB1; Fig. 2; Fig. S1d, Supporting Information) at near daily-intervals over six days were: 600, 50, 5, no attempt, 150 and 0 ml. Brine volumes collected from the newly installed pipe (accessing CB3; Fig. 2) over the last three days were: 50, 300 and 20 ml. At each sampling, the maximum volume was removed, indicating recharge between most samplings. Brines from CB1 and CB3 were collected from 1.3 and 1.0 m below the permafrost tunnel floor, respectively (Fig. 2). No liquid brine was encountered in either the newly drilled hole (IA; Fig. 2) or while coring the ice wedge (IWC; Fig 2.). Brine pH was between 7 and 7.5. The volume of the brine reservoir is unknown, though our sampling efforts suggested numerous low volume (<1 L mobile liquid) pockets of loosely connected brine.

Salinity and major ions

Brine salinity, calculated from conductivity measurements, was 115 ppt for brine recovered from both CB1 and CB3. Salinity of

the melted ice core sections averaged 0.04 ± 0.01 ppt with no apparent trend in conductivity with depth (data not shown). Chloride, sodium, magnesium, sulfate, calcium, ammonium and potassium accounted for the majority of ions in the cryopeg brine (listed here in order of abundance; Table 1). Considering these dominant ions and using Grant's (2004) equation, water activity (a_w), of these brines was 0.93, which falls within the range for microbial activity and growth (Grant 2004).

Stable isotopes

Oxygen isotope values tended to increase with depth in the ice wedge core, ranging from –27.7‰ to –23.2‰, but the highest $\delta^{18}O$ values of –21.0‰ to –21.4‰ were obtained from the brine (Fig. 3). DE values for the ice sections ranged between 4.1‰ and 11.7‰ and also tended to increase with depth, while DE values of –0.8‰ and –4.0‰ for the brine were significantly lower (unpaired *t*-test, $P = 0.0001$; Fig. 3).

Particulate matter variables

Concentrations of all measured particulate variables were notably higher in the cryopeg brines than in the ice wedge core. Total SPM averaged only 0.30 ± 0.16 mg ml^{-1} ice melt (Fig. 4a). SPM was not quantified in the cryopeg brines (to conserve volume for other purposes) but, based on observations while filtering

Table 1. Comparative concentrations (mM) of major ions in cryopeg brines, Standard seawater and the Barrow ice wedge (na indicates data not available).

	Cryopeg brines					
Ion	Lake Yakutskoye[a]	Cape Chukotsky[a]	Varandei Peninsula[b]	Barrow	Standard seawater	Barrow ice wedge[c]
Ammonium	na	na	na	38.1	*[d]	0.1 (0.1)
Bromide	na	na	na	2.7	0.8	0.0 (0.0)
Calcium	30	40	8.9	52.4	10.3	0.3 (0.0)
Chloride	2630	1940	111	1930	546	0.8 (0.1)
Fluoride	na	na	na	3.3	68	0.1 (0.1)
Magnesium	310	195	28.5	357	52.8	0.2 (0.1)
Nitrate	na	na	na	0	*	0.0 (0.0)
Nitrite	na	na	na	0.1	*	0.0 (0.0)
Phosphate	na	na	na	0.4	*	0.0 (0.0)
Potassium	20	10	6.2	23.5	10.2	0.1 (0.0)
Sodium	2000	1520	99.5	1680	469	0.7 (0.1)
Sulfate	35	31.5	23.8	64.4	28	0.1 (0.0)

[a]Data from Gilichinski *et al.* 2003, [b]Data from Pecheritsyna *et al.* 2007, [c]Mean (±S.D.) values for measurements on 13 ice core sections, [d]Microbially cycled ions that vary over orders of magnitude spatially and temporally in the ocean.

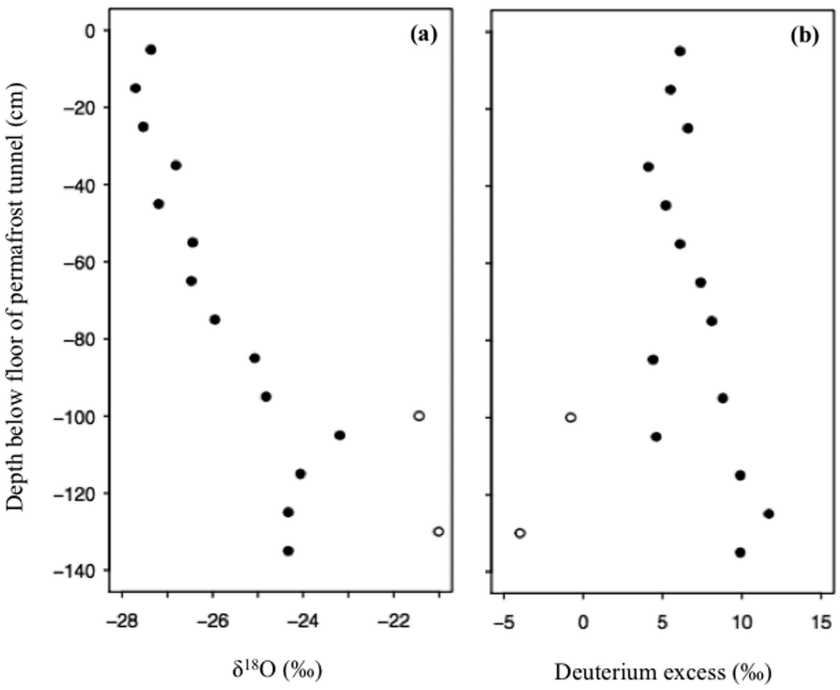

Figure 3. Depth profiles of oxygen isotope measurements (**a**) and calculated DE (**b**) for the cryopeg brines and ice wedge core sections. Standard deviations for triplicate measurements of brine (open symbols) and ice sections (closed symbols) were <0.2‰ for $\delta^{18}O$ and <2‰ for $\delta^{2}H$.

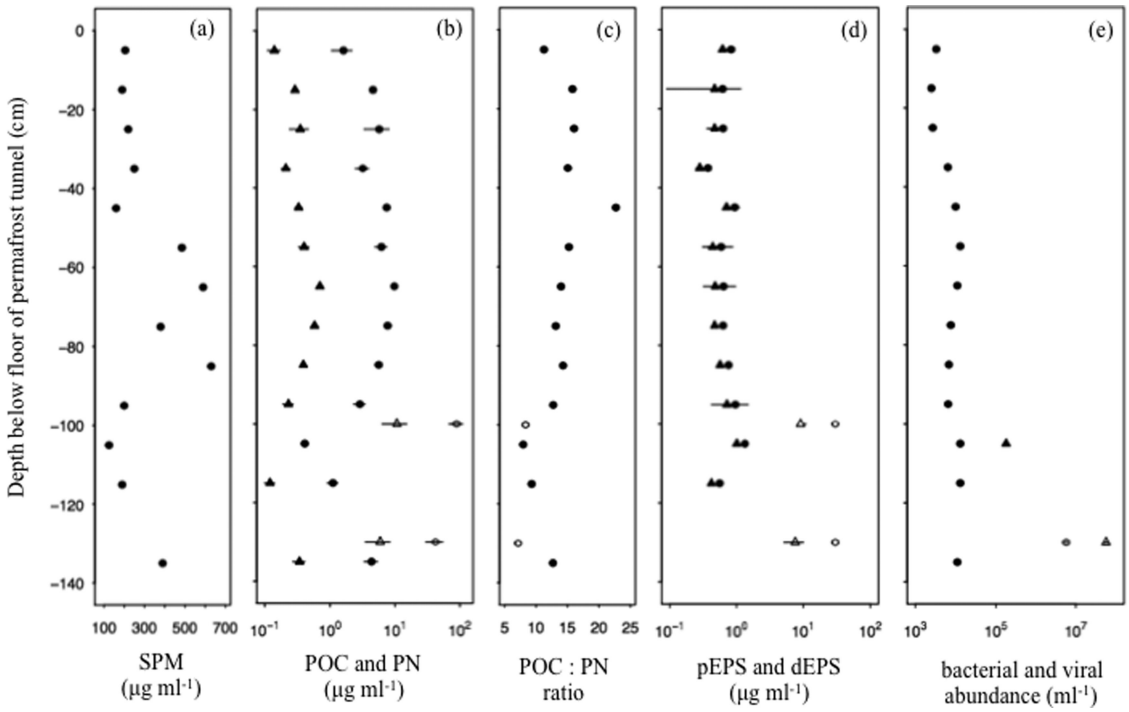

Figure 4. Depth profiles of particulate parameters for the cryopeg brines and ice wedge core sections. Measurements on cryopeg brines (open symbols) and ice sections (closed symbols) are shown for (a) SPM, (b) POC (circles) and PN (triangles), (c) POC:PN ratio, (d) EPS in particulate (pEPS, circles) and dissolved (dEPS, triangles) form and (e) abundance of bacteria (circles) and viruses (triangles).

comparable volumes of brine and ice melt for other purposes, was at least several-fold greater. Filtered material from CB1 brine was bright orange in color and appeared viscous without visible structure (a cohesive, pliable mass on the filter) in contrast to SPM from the ice sections, which was brown and appeared to be composed of sediment grains and decomposing plant matter (Fig. S2, Supporting Information). Cryopeg POC was 42 and 89 μg ml^{-1} (CB1 and CB3, respectively), 10—20-fold greater than the mean concentration in the ice sections (4.5 $\pm$ 2.7 μg ml^{-1}), while PN was 5.9 and 10.7 μg ml^{-1} in the brines, 20—35-fold the mean concentration in the ice (0.31 $\pm$ 0.18 μg ml^{-1}; Fig. 4b). The C:N ratios of 7.2 and 8.4 in the brines were lower than any ratio measured in the ice save one, where the average ratio was 13.8 $\pm$ 3.5. An even greater contrast between the brine and ice samples was found for particulate and dissolved forms of EPS: brine pEPS was between 30 and 42 (CB1), and between 30 and 89 μg C ml^{-1} (CB3), compared to 0.4–1.3 μg C ml^{-1} ice melt, and brine dEPS was 7.6 $\pm$ 2.4 (CB1) and 9.1 $\pm$ 0.2 μg C ml^{-1} (CB3), compared to 0.3–1.0 μg C ml^{-1} in ice melt (Fig. 4d). Given the very low salinities of the ice wedge samples, EPS was not scaled to brine volume as is done for sea ice with its higher brine content (Krembs *et al.* 2002).

Bacterial and viral abundance

DAPI-stained fluorescing bacteria in cryopeg brine outnumbered those in the ice sections by nearly three orders of magnitude: 5.7 $\pm$ 0.3 $\times$ 10^6 cells ml^{-1} (n = 2 technical replicates) versus 8.5 $\pm$ 3.9 $\times$ 10^3 cells ml^{-1} (n = 13; Fig. 4e). The abundance of VLP in the brine was also much higher than in the ice wedge: 5.7 $\pm$ 0.5 $\times$ 10^7 ml^{-1} (n = 2 technical replicates), versus 1.8 $\pm$ 0.3 $\times$ 10^5 ml^{-1} (n = 2 technical replicates from ice wedge core section 100–110 cm), making the virus–bacteria ratio in the two environments markedly different: 10 and 1.4 in brine and ice, respectively. Enumeration of both VLP and bacteria from CB3 was confounded by high background fluorescence. Epifluorescent images of cryopeg brines captured bacteria reproducing (dividing cells), while no such events were seen in ice core sections. TEM images of 0.2 μm filtered brine confirmed the identity of fluorescing particles below that size threshold as bacteriophage, in particular those identifiable as Siphoviridae (Fig. 5). Although specific methods to identify protists were not employed, no protists were observed microscopically (similarly to winter sea ice; Deming 2010).

Viral metagenome

Sequencing of the viral metagenome (virome) yielded 227 899 sequences, with an average read length of 363 bp and 45% GC content. Comparative rarefaction curves between the cryopeg virome and similar environmental virome datasets (hypersaline, marine sediment, freshwater, seawater; equally sampled to 50 000 sequences) showed the cryopeg virome to approach saturation of unique sequences at a lower number of reads (Fig. 6). From a BLASTx comparison with the NCBI Refseq database of complete viral genome protein sequences (2014.09.10 release) for taxonomic composition, 31% of the Barrow cryopeg virome sequences presented a significant hit (BLAST bitscore threshold of 50). Of these hits, taxonomic composition was nearly entirely (95%) dsDNA viruses, and these were dominated by Caudovirales (85% of viral proteins; Fig. S3, Supporting Information). Notably, when compared to 113 other viromes from other aquatic or extreme environments, including marine sediments (n = 12), freshwater (n = 31), seawater (n = 60) and hypersaline, desert, or thermophilic settings (n = 16) (Metavir database; http://metavir-meb.univ-bpclermont.fr/), the cryopeg brine virome had a higher percentage (30%) of homologous sequences (to Refseq) than all but two of the viromes queried (mean of 10 $\pm$ 8%, n = 111; Table S1, Supporting Information). More than 40% of identified reads in the cryopeg virome had greatest similarity to

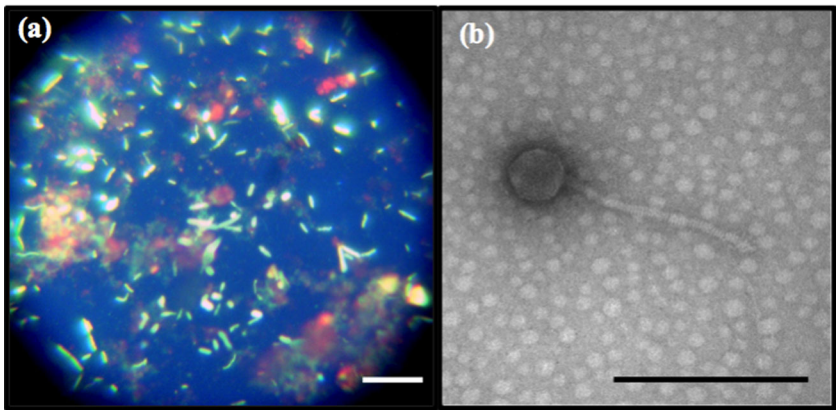

Figure 5. Microscopic images of bacteria and viruses in cryopeg brine. Bacteria were stained with DAPI and observed by epifluorescence microscopy using a Zeiss LP420 emission filter; scale bar is 20 μm (a). Viruses were confirmed by transmission electron microscopy, as exemplified by this Siphoviridae bacteriophage; scale bar is 200 nm (b).

13 viruses of phylogenetically disparate hosts, including *Bulkholderia* phages (AH2, BcepNazgul and BcepC6B at 10%, 5% and 2%, respectively), *Loktanella* phage pCB2051-A (4%), deep-sea thermophilic phage D6E (4%), *Providencia* phage Redjac (3%), *Enterobacter* phage Enc34 (3%), *Pseudomonas* phage YuA (2%), *Clostridium* phage phi3626 (2%), *Pseudomonas* phage B3 (2%), *Salmonella* phage FSL SP-088 (2%), *Bacillus* phage PBC1 (2%) and *Nitrincola* phage 1M3-16 (2%; Table S2, Supporting Information). Ten of these 13 viruses are either temperate (identified as prophage experimentally), likely temperate, (presence of known integrase and repressor genes) or possibly temperate (viral genes originating from these viruses found in microbial genomes). Sequences with greatest homology to microbial genes were phylogenetically most similar to members of the phyla Gammaproteobacteria, Clostridia and Alphaproteobacteria, and disproportionately to the genera *Clostridium* (17%), *Marinobacter* (5%) and *Bacillus* (4%). Sequences ascribed to microorganisms may be due to incomplete representation of viral genes in databases used for comparison, unidentified prophages annotated as microbial in origin, or microbial host genes incorporated into viral genomes (any microbes <0.2 in size and still present in the cryopeg brine filtrate would have been lysed and the released DNA degraded by procedures used prior to extracting the viral DNA). The cryopeg viral genes with annotated function that were present in greatest abundance coded for coat proteins, portal proteins, terminases and integrases (collectively 15%; Table S3, Supporting Information). Interrogation of the cryopeg virome for viral marker genes (AVS, G20, GP23, MCP, PhoH, PolB, PolB2, PsbA, RdRP, Rep, T7gp17, TerL and VP1) yielded homologous sequences to only two of these 13 genes: PhoH (2 sequences) and TerL (332 sequences). Paired-comparison of similarity (Bray–Curtis dissimilarity indices) between the cryopeg virome sequences and 50 other environmental viromes (curated from the larger set of 113 to avoid hyper-redundancy in some environments) demonstrated its unique composition, among all of the viromes, and closest similarity to desert and hypersaline environments (Fig. S4, Supporting Information).

DISCUSSION

Seawater origin of Alaskan cryopeg brine

Several lines of evidence indicate that the cryopeg brines near Barrow are thalassohaline. The first line is based on the similarity of major ions in the cryopeg brine to those in Yakutskoye Lake and Cape Chukotsky cryopeg brines, suggestive of similar source and formation processes, and on the substantial dissimilarity to ion concentrations in the ice wedge core (Table 1). The mass ratio of SO_4^{2-} to Cl^- for the Barrow cryopeg brine was 0.09, which represents a significant depletion of sulfate relative to Standard seawater (0.14; Millero *et al.* 2008), but is higher than the ratio for Siberian cryopeg brines (0.04) shown to be of marine origin (Gilichinsky *et al.* 2003; Table 1). Depletion in sulfate relative to seawater has been reported for sea ice and brine (Meese 1989; Maus *et al.* 2011). Cooling of brine below the precipitation point of mirabilite ($NaSO_4 \bullet 10\ H_2O$) at roughly –8 °C (Marion and Kargel 2008) results in sulfate removal and potential fractionation through immobilization of the precipitate. This cooling effect is in line with observed brine temperatures in Yakutskoye Lake and Cape Chukotsky cryopegs that fall below the mirabilite precipitation point. Some higher sulfate fractions for data from Barrow may be indicative of fractionation during colder periods in the thermal history of the brines. Brines from the Varandei peninsula are much less saline, with a SO_4^{2-}:Cl^- ratio of 0.55, and have likely undergone a complex evolution that precludes direct comparison with the other ion data sets (Table 1).

The second line of evidence for a marine origin derives from stable isotope analyses. Compared to the cryopeg brine $\delta^{18}O$ values (–21.0‰ and –21.4‰), Barrow sea ice $\delta^{18}O$ values are much higher, ranging between –2‰ and 1‰, while overlying snow values typically range between –18‰ and –30‰ (Eicken et al. 2004, 2012; Meyer *et al.* 2010). Based on low $\delta^{18}O$ values, Meyer *et al.* (2010) concluded that ice wedges in permafrost near Barrow were of meteoric and non-marine origin, deposited at a time of lower air temperatures and greater distance to moisture sources, with some potential changes due to subsequent fractionation and interaction with soil minerals in melt–freeze cycles. However, low $\delta^{18}O$ values alone do not preclude marine origin. Ice growing from water or brine due to fractionation would have a $\delta^{18}O$ higher than the source liquid by typically 1 to 2.5 ‰ (depending on ice growth rate; Eicken 1998). Our hypothesis of different source waters and freezing paths for the brine and ice wedge is supported by the relative proportion of ^2H and ^{18}O in the samples. The fractionation of atmospheric precipitation results in a linear relationship between δ^2H and $\delta^{18}O$ (meteoric water line, MWL); condensation/freezing processes that differ from Rayleigh fractionation in the atmosphere do not fall on the MWL

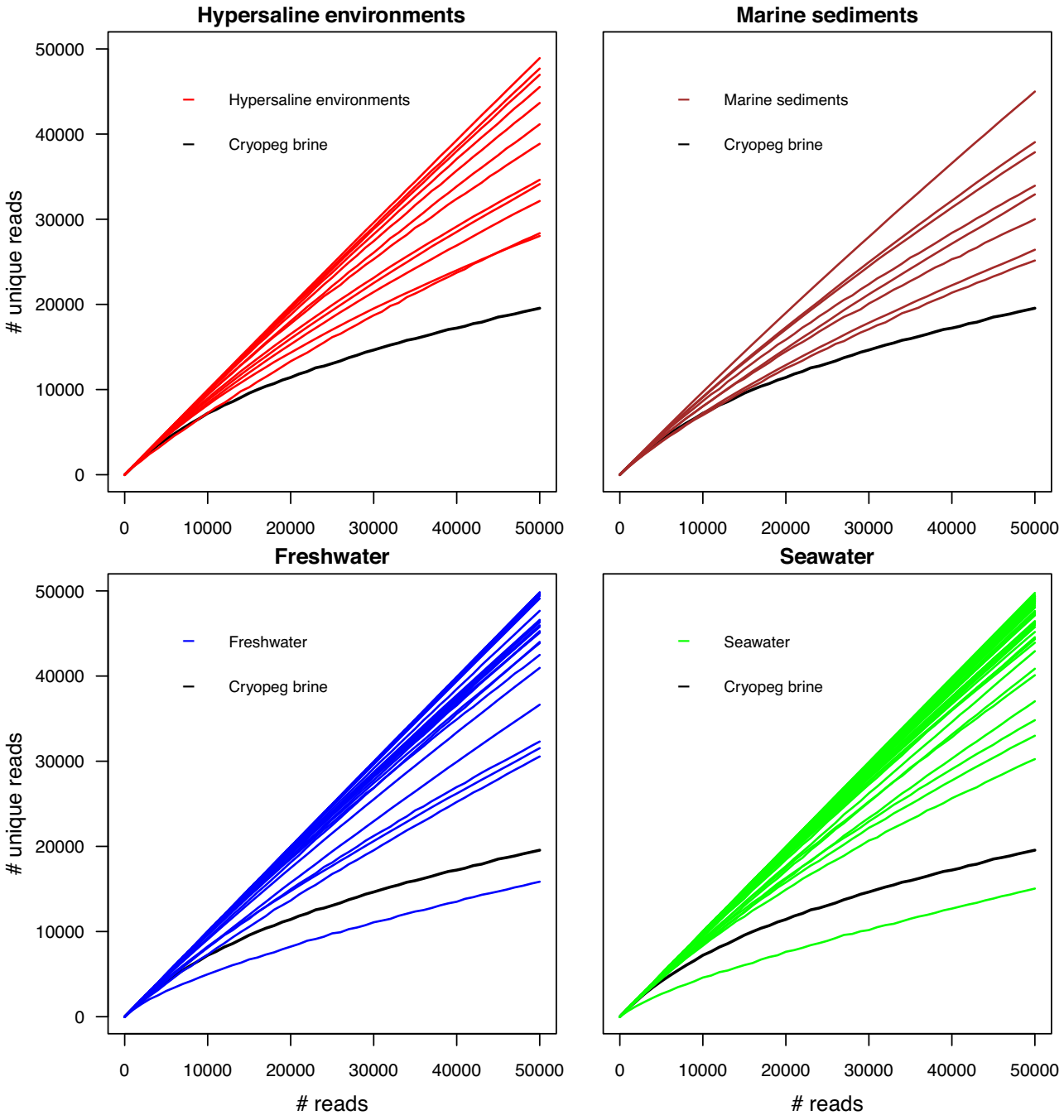

Figure 6. Comparative rarefaction curves for Barrow cryopeg brine and 100 other environmental viromes. These viromes are listed in Table S1 (Supporting Information), and metadata are available at MetaVir2.0 (http://metavir-meb.univ-bpclermont.fr/).

(Craig 1961). DE shows the deviation of our samples from the MWL (Fig. 3): the cryopeg brine values fall outside those for the ice wedge core indicating a separate fractionation history. This discrepancy in DE values between the brine and ice core indicates that a significant part of the brine is derived from seawater that fractionated as it migrated and evolved over time through sequential freezing. However, as demonstrated in a modeling study, corroborated by field data (Eicken 1998), Rayleigh fractionation in a semi-enclosed system such as sea ice can generate brine $\delta^{18}O$ compositions that fall well below those of standard seawater, with values of –10 ‰ and lower. Such sequential fractionation of the source water subjected to low temperatures is in line with observed depletion of sulfate relative to chloride in the cryopeg brine.

Third, sequence analysis of the cryopeg brine virome supports a seawater origin. A high proportion (5%) of all of the genes identified in the virome was most similar to genes identified from *Marinobacter* (e-value cutoff 10^{-5}). *Marinobacter* is a genus of Proteobacteria isolated exclusively from seawater and marine and estuarine sediments, and 16S rRNA genes most similar to those of *Marinobacter* have been found in deep sea and coastal sediments, hypersaline mats, hydrothermal vents and sea ice

(Duran 2010). The most likely sources of these genes in the cryopeg virome are viruses of *Marinobacter* hosts, organisms that would have entrained with the original source water of marine origin.

Overall, the regional geologic history also supports the scenario of a marine origin for sediments of the Barrow peninsula. Following the marine transgression during the last interglacial, with a coastal lagoon covering the area of the sampling site (Brigham-Grette and Hopkins 1995), sediments were gradually exposed. During this period, mixing of marine and meteoric waters was likely, but sampling in the region suggests that gradual closure of a coastal lagoon (Brown 1969) with production of brines *in situ* was equally plausible. Each of these processes, individually or in combination, would result in sequential cooling and potential migration of the sub-freezing brines. Mixing of meteoric and marine source waters, e.g. during the ice wedge formation episodes dated to roughly 14 Ka ago by Meyer *et al.* (2010), adds to the combination of geochemical, isotopic and gene-based findings that support a marine origin for the Barrow cryopeg system.

Cryopeg brine as an EPS-rich microbial habitat

EPS produced in sea ice is attributed primarily to ice algae (Krembs *et al.* 2002; Underwood *et al.* 2013); in upper zones of dark winter sea ice, however, where diatoms are excluded physically or are inactive, EPS production has been attributed to bacteria (Collins, Carpenter and Deming 2008). For both ice algae and bacteria, EPS serve as cryoprotectant and osmoprotectant, enhancing tolerance of freeze–thaw conditions and high salt concentrations (Krembs *et al.* 2002, Krembs, Eicken and Deming 2011; Liu *et al.* 2013). No diatoms were detected microscopically in this cryopeg brine, nor is their presence anticipated given the absence of light over geological time; the EPS detected in the brine is thus assumed to be of bacterial origin. A caveat is that fungi have been cultured from Siberian cryopegs originally at sub-zero temperatures (–2°C) and high salinity (10%; Kochkina *et al.* 2007), though they have not been shown to be active under *in situ* conditions nor to produce EPS. As we did not evaluate their presence, a fungal contribution to the measured EPS cannot be excluded.

The Barrow cryopeg brines harbor EPS concentrations within the ranges found in other sub-zero brines for which comparable data are available; i.e. brines associated with sea ice (Table 2). The dominance of pEPS over dEPS (77–80% versus 9–23% of total EPS) in cryopeg brine, however, is opposite that found in bottom sea ice brines, where dEPS dominates and pEPS accounts for only 17–42% of the total EPS (Krembs, Eicken and Deming 2011). In brine-wetted snow on the surface of sea ice, pEPS concentrations are low (0.1–0.2 μg C ml^{-1}) and account for an even smaller percentage (6%) of the total (Ewert *et al.* 2013), similar to that found in Arctic winter sea ice (Table 2). Briny frost flowers on the bare surface of new sea ice have the lowest percentages of pEPS (1–7%; Barber *et al.* 2014). These differences persist despite the various brines having similar salinity, temperature and bacterial concentration; for example, upper winter sea ice brine at 158 ppt and –12 °C with 7.2 × 10^6 bacteria ml^{-1} contained 5.6 mg pEPS C L^{-1} (Ewert *et al.* 2013), while Barrow cryopeg brine at 115 ppt and –6 °C with 5.7 × 10^6 bacteria ml^{-1} (CB1) contained 30–42 mg pEPS C L^{-1}. These differences in concentration and relative fractions of pEPS and dEPS between cryopeg and sea ice-associated brines indicate differences in the production and degradation of EPS.

In terms of EPS production, the particulate C:N ratios of 7.2–8.4 found in the cryopeg brine are consistent with an active microbial community (as also evidenced microscopically; see below), producing nitrogen-containing pEPS (Mancuso Nichols *et al.* 2004). In contrast, the higher ratios in the ice wedge core (8.0–16.1; Fig. 4c) reflect more recalcitrant organic material present only at low levels in this ice, where bacterial abundances were also very low. The cryopeg C:N ratios are comparable to those from the most biologically active zones in sea ice (e.g. 7.2–8.7; Krembs, Eicken and Deming 2011), yet a differential degradation of the EPS is apparent. The pattern of a high percentage of dEPS in brines exposed to sunlight and a low percentage in the permanently dark cryopeg brines suggests the involvement of UV-B driven photolysis in degrading EPS (Bowman and Deming 2010) and the absence of this forcing in cryopegs. The microbial benefits that would accrue from high amounts of pEPS in the cryopeg include not only cryoprotection and osmoprotection (Krembs *et al.* 2002; Liu *et al.* 2013) but also physical (viscous) support for the metabolic exchanges and symbioses that characterize anoxic environments (Decho 1990; Boetius *et al.* 2000; Wrede *et al.* 2013) and possible protection against viral infection (see below). The much lower amounts of dEPS in the cryopeg brine can be explained by bacterial metabolism of dEPS as they become available.

To deduce pEPS and dEPS processes from a snapshot of data, we considered published rates and conversion factors to estimate turnover times for both size classes of EPS. For pEPS production, we used the rate of pEPS accumulation in sea ice at a comparable cryopeg temperature (35 ng C ml^{-1} d^{-1} at –5 °C; Krembs *et al.* 2002), the available rate of bacterial pEPS production in seawater (2.04 fg C cell^{-1} d^{-1}, albeit at 20 °C; Stoderegger and Herndl 1998) and the carbon:pEPS conversion factor (0.75; Engel and Passow 2001) used by Krembs *et al.* (2002). The maximal pEPS production rate calculated for the bacterial population size in our cryopeg samples was 12 ng C ml^{-1} d^{-1}. Assuming steady state, this pool of pEPS would turn over in 46 years. Production of dEPS by bacterial communities has not been quantified, but a rate of 60 fg C cell^{-1} d^{-1} was measured at 2°C for the model marine psychrophile *Colwellia psychrerythrea* 34H (Ewert 2013). Applying this rate to the cryopeg bacterial community yielded 354 ng C ml^{-1} d^{-1}, indicating turnover of the dEPS pool in 2.4 years. This order of magnitude difference between the residence times of pEPS and dEPS in the cryopeg brine is consistent with the use of pEPS for protection against various stressors (and the absence of photolysis as a breakdown mechanism) and the consumption of dEPS for metabolism. An alternative explanation for unusually high ratios of pEPS to dEPS in the brine would invoke the re-charge process that occurred between sampling events; however, any selective retention of EPS in permafrost during brine seepage would have favored pEPS, resulting in a higher fraction of dEPS in the brine (as observed in brine seeping from sea ice into overlying snow; Ewert *et al.* 2013), when the opposite was observed.

Another role for EPS is to complex heavy metals, especially in microbial biofilms (Guibaud *et al.* 2005), and to sequester metals in general (Mancuso Nichols, Guezennec and Bowman 2005). Cadmium and lead were 60- and 200-fold greater in the Barrow cryopeg brines than in seawater (K. Yoshikawa, pers. comm.), suggesting this additional benefit of EPS to the cryopeg microbial community. Given the lack of color and relative transparency of cryopeg brine upon collection, and the color change to orange upon exposure to air (Figs S1 and S2, Supporting Information) indicating iron oxidation, the cryopeg brine must have also contained reduced forms of iron and thus be anoxic in situ. The color of brines exuding from Blood Falls in Antarctica displays similarly due to the presence of hydrated iron oxides and silt

Table 2. Comparative characteristics (range of values) for aqueous, subzero, hypersaline microbial habitats. Particulate EPS (pEPS), bacteria and VLP values are scaled to brine volume. Values for pEPS reported by cited authors as Xanthan gum eq. were multiplied by 0.75 to convert to C; values reported as Glucose eq. were multiplied by 0.4 (as in Krembs, Eicken and Deming 2011). dEPS indicates dissolved EPS; na indicates data not available.

Habitat	Temperature (°C)	Salinity (ppt)	pEPS (μg C ml^{-1})	dEPS (% total EPS)	Bacteria (no. ml^{-1})	VLP (no. ml^{-1})	References
Cryopeg brine, Barrow, Alaska	−6	115	30–89	9–23	5.7×10^6	5.7×10^7	This study
Brine-wetted snow[a] on Barrow winter sea ice	−18 to −6	80–184	0.2–0.5	94	$1.2–2.6 \times 10^4$	na	Ewert *et al.* (2013)
Frost flowers on Arctic sea ice	−13 to −7	66–114	0.14–0.18	93–99	$1.6–4.5 \times 10^5$	$0.2–1.2 \times 10^5$	Barber *et al.* (2014)
Sea-ice brines[b], Arctic winter	−18	190	60	na	3.3×10^6	na	Krembs *et al.* (2002)
	−30 to −24	231–236	na	na	$4.6–15 \times 10^6$	$2.4–8.2 \times 10^7$	Wells and Deming (2006c)
	−26 to −15	180–230	0.8–75	na	$0.42–20 \times 10^7$	na	Collins, Carpenter and Deming (2008)
	−25 to −11	125–205	0.3–1.42	78–94	$4.0–8.4 \times 10^5$	na	Ewert *et al.* (2013)
Sea-ice brines, Arctic spring	−2[c]	38[c]	na	na	$0.13–8.3 \times 10^7$	$0.8–13 \times 10^8$	Maranger, Bird and Juniper (1994)
	−10	135	95	na	8.9×10^6	na	Krembs *et al.* (2002)
Sea-ice brines, Arctic fall	−11 to −5	83–153	na	na	$1.8–9.2 \times 10^5$	$0.055–1.7 \times 10^9$	Collins and Deming (2011)
Sea-ice brines, Antarctic fall–spring	−6 to −2	47–100	na	na	$0.39–3.3 \times 10^5$	$0.6–3.5 \times 10^5$	Paterson and Laybourn-Parry (2012)
Hypersaline springs at Lost Hammer, Axel Heiberg	−6 to −5	220-260	na	na	$0.27–2.2 \times 10^5$	$1.7–5.3 \times 10^5$	Colangelo-Lillis, Wing and Whyte (2016)
Subglacial brine from Taylor Glacier, Blood Falls	−8 to −5	80–88	na	na	na	na	Keys (1979)
	na	na	na	na	$0.1–7.6 \times 10^5$	na	Mikucki and Priscu (2007)
Ace Lake, Antarctica	−40 to 13	7–43	na	na	na	na	Rankin *et al.* (1996)
	na	18	na	na	$0.8–1.6 \times 10^6$	$0.9–6.1 \times 10^7$	Madan, Marshall and Laybourn-Parry (2005)
Lake Vida, Antarctica	−13	188	na	na	$1.0–6.0 \times 10^5$	$4.9–6.0 \times 10^7$	Murray *et al.* (2012)

[a]2-cm snow layer above sea ice surface, [b]Surface ice (0–10 cm below surface) or uppermost horizon reported, [c]These values were assumed, based on information in Maranger, Bird and Juniper (1994), in order to scale values for bacteria and VLP to brine volume, using the equations of Cox and Weeks (1983).

(Keys 1979). While the orange particulates filtered from the brine (Fig. S2, Supporting Information) were not analyzed chemically, their appearance is consistent with oxidized iron embedded in a mass of pEPS. The detection of *Marinobacter* genes in the cryopeg virome (see above) may also be relevant, as this genus includes anaerobic Fe-oxidizing chemoautotrophs (Edwards *et al.* 2003). The high abundance and likely source and utility of different size classes of EPS in cryopeg brines expand the importance of EPS in protecting and sustaining microbial communities in sub-zero hypersaline habitats, from sunlit oxygenated sea ice environments to dark anoxic cryopeg brines.

Viral evidence for an active microbial community

The ratio of virus-like particles (VLP) to bacteria found in the cryopeg brine (Canfield *et al.* 2013) matches the ratio most frequently reported from seawater and commonly interpreted as evidence for an active microbial community (Wommack and Colwell 2000). This ratio has been shown to be significantly related to bacterial turnover in samples from deep Mediterranean sediments (Danovaro, Manini and Dell'Anno 2002), wherein bacterial hosts are regularly infected and lysed. We considered potential viral dynamics in the cryopeg brine based on data from this study and the literature, particularly from work on viral dynamics at conditions as close as possible to cryopeg brines. Using the viral burst size (55 virions per host cell) and latent period (5 h) determined at –1 °C and 35 ppt by Wells and Deming (2006a) and the viral decay rate (1% d^{-1}) determined at –12 °C and 160 ppt (Wells and Deming 2006b), we calculated that 0.04% of bacteria in the brine must be infected to maintain the detected viral population at steady state. To maintain the measured bacterial population size, the bacterial growth rate must be 7.5×10^{-5} h^{-1} and the contact rate between viruses and bacteria must be 7.5×10^{-5} contacts $cell^{-1}$ h^{-1}, assuming 100% of contacts result in successful infection and lysis. Using the contact frequency equation of Murray and Jackson (1992; see Table 3), and the least-squares best-fit equation for brine viscosity at low temperature and high salinity (Collins and Deming 2011), the modeled contact rate is 7.7×10^{4} contacts cm^{-3} h^{-1}, or 0.13 contacts $cell^{-1}$ h^{-1}, four orders of magnitude greater than calculated for the steady-state scenario. This result suggests that the large majority of modeled contact events are by non-infective viruses, are between viruses and non-hosts, or result in lysogeny not host lysis. It further suggests that cell adsorption is a more important mechanism for viral inactivation in this extreme environment than viral decay, given that virions will contact a bacterium before decaying.

Calculated contact rates rely on a number of assumptions, but the rates lead to testable hypotheses. Of particular interest is the likelihood that many viral infections in sub-zero brines are of a non-lytic nature (Boetius *et al.* 2015); a correlation between lysogenic replication and increasing salinity was demonstrated several decades ago (Wais and Daniels 1985). The cryopeg virome indicates that a substantial fraction of viruses in the cryopeg brine are capable of lysogenic replication. A high frequency of temperate phage increases the potential for lateral gene transfer, which could explain the detection of *Marinobacter* genes in the cryopeg virome. DeMaere *et al.* (2013) noted high levels of intergenera gene exchange between haloarchea under cold high-salinity conditions of an Antarctic lake, which they proposed as conditions especially suited for lateral gene transfer.

The disproportionate presence of pEPS in the cryopeg brines may also provide a defense against viral infection. Its presence would influence viral diffusivity (Table 3) and reduce the contact rate between virions and potential hosts. Given the correlation between number of VLP we observed and number of infective virions in a model system under temperature and salinity conditions similar to this cryopeg (Wells and Deming 2006a), the majority of cryopeg virions may be infective, increasing the benefits of a viral defense mechanism. Although viruses have been found in every environment examined for their presence, surprisingly few sub-zero hypersaline environments have been evaluated for this basic and influential component of microbial ecosystems (Table 2).

Microbial refuges in the face of global-scale surface alteration

Isolated from surface processes that would normally result in seasonal temperature and salinity fluctuations, driven by wind, current or atmospheric conditions (Ewert and Deming 2013), and in mixing through percolation and perfusion with extraneous liquid, the sub-surface temperature and salinity regime of cryopeg environments is expected to be more stable than cold and hypersaline surface environments (Table 2). Microbial habitats with stable physical and chemical conditions are less biologically resistant to perturbation and less conducive to driving biological innovation and diversity (Girvan *et al.* 2005); they are instead expected to preserve life, even when environmental conditions appear to be extreme.

The modeled size of water films in ice wedges and permafrost (<10 nm for the temperature range discussed here; Anderson 1967; Dash, Rempel and Wettlaufer 2006) greatly limit

Table 3. Equations, variables and values used to calculate virus-bacteria contact rates.

Equations and variables	Definition	Value	Units
$J = 2\,\pi\,d_c\,D_v\,V\,B$	Virus–bacteria contact rate equation	2.2×10^{1}	$cm^{-3}\ s^{-1}$
$D_v = k\,T / 3\,\pi\,\mu\,d_v$	Viral diffusivity equation	2.4×10^{-10}	$cm^{2}\ s^{-1}$
$\mu = (10.2 - 0.00132S - 0.0835T + 0.000177T^2)^{-1}$	Brine viscosity equation	2.7×10^{0}	$g\ cm^{-1}\ s^{-1}$
d_c	Diameter of average cell	5.0×10^{-5}	cm
D_v	Viral diffusivity	2.4×10^{-10}	$cm^{2}\ s^{-1}$
V	Virus concentration	5.7×10^{7}	cm^{-3}
B	Bacteria concentration	5.7×10^{6}	cm^{-3}
k	Boltzmann constant	1.4×10^{-16}	$g\ cm^{2}\ K^{-1}\ s^{-2}$
T	Temperature	2.7×10^{2}	K
μ	Brine viscosity	2.7×10^{0}	$g\ cm^{-1}\ s^{-1}$
d_v	Diameter of average virus	6.0×10^{-6}	cm
S	Salinity	1.2×10^{2}	ppt

or prevent diffusion of viruses and cells between the cryopeg brine system and surrounding permafrost. Considering this effective physical isolation, and in the absence of microbial genomic characterization, we propose (like others, referenced earlier for work on Siberian cryopegs) that the bacterial inhabitants of Barrow cryopegs are primarily ancestors to marine organisms selected to adapt to a radically different environment as the brine was isolated from the ocean, and then from light and the atmosphere. The isolation effect is reflected in the limited diversity of the cryopeg virome relative to other contemporary habitats regularly exposed to environmental fluctuations. How long such an isolated system can persist is dependent on the geochemical processes that supply chemolithoautotrophs with metabolic substrates and the rates of activity and growth by the heterotrophic community. Although our work does not constrain these processes or rates, it has revealed the presence of similar aqueous chemistry to other cryopeg brines and the brines of Lake Vida and Blood Falls, which support a variety of autotrophs and heterotrophs via endogenous and allochthonous organic carbon, and sulfur and iron oxidation (Gilichinsky et al. 2003, 2005; Mikucki and Priscu 2007; Murray *et al.* 2012). While cryopegs have been isolated for tens to hundreds of thousands of years, the Antarctic Blood Falls reservoir brine has been inhabited for over one million years since its physical isolation. Cryopeg systems offer an alternative Arctic window into ancient marine microbial communities and more accessible sites for exploring community change in response to possible future changes in energy and nutrient sources with climate warming.

Sub-surface environments like cryopegs may serve as microbial refugia during large-scale shifts in Earth's surface temperature or atmospheric chemistry, as in Snowball Earth episodes (Hoffman 1998) or periods of oceanic and atmospheric oxidation or reduction (Canfield *et al.* 2013). Similar isolation events may have occurred on the surface of Mars as its water and atmosphere were lost (Pollack *et al.* 1987), driving any surface life to extinction or sub-terranean existence (Ehlmann *et al.* 2011). Such sub-surface environments are targets for future efforts to find extraterrestrial biosignatures (McKay *et al.* 2013). Further investigating the genomics and geochemistry of terrestrial analog systems may inform this search for sub-surface microbial life elsewhere.

CONCLUSIONS

The Barrow Permafrost Tunnel cryopeg system appears to be of different origin and in strong compositional and microbiological contrast with its neighboring ice wedge. Analyses of ions, stable isotopes and viral genes indicate a separate, marine origin for the cryopeg brines. Further work is required to evaluate the age and evolution of these brines, thought to originate from sequential enclosure and isolation of coastal or estuarine water bodies. The cryopeg brines contain relatively high concentrations of viruses and EPS explained by the presence of active bacteria. The limited viral diversity points to the stability of the cryopeg and its isolation from surface environments. The high ratio of pEPS to dEPS likely reflects the protective benefits of pEPS to microbial inhabitants of this extreme environment, regardless of physiology, and the heterotrophic consumption of dEPS.

Enclosed sub-zero hypersaline environments are uncommon and rarely reported in the literature. This study, by providing a snapshot of processes occurring within a cryopeg, establishes a foundation for exploring anaerobic metabolisms under extreme conditions and viral–bacterial dynamics in a subterranean environment of marine origin that differs from the oceanic realm. This cryopeg system may also serve as a useful analog environment for anoxic refugia for life from even more extreme conditions during Earth history, or on other planets and moons in the solar system, and offer a unique window into evolutionary processes in such an isolated habitat. The Barrow cryopegs and similar systems have an unknown future: while we document this system as ancient and isolated, the Arctic is undergoing rapid and substantial change. As the potential for surface freshwater invasion into sub-surface permafrost layers increases with climate change, this cryopeg system will be less isolated from surface and atmospheric processes. Further exploration is warranted to learn what we can from this and similarly shallow cryopegs before their inhabitants merge with or are displaced by overlying contemporary microbial communities.

SUPPLEMENTARY DATA

Supplementary data are available at FEMSEC online.

ACKNOWLEDGEMENTS

Mette Kaufman's help in the laboratory and Tom Douglas' support in providing access to his ion chromatography lab are gratefully acknowledged. Kenji Yoshikawa kindly helped with securing access to the permafrost tunnel and by sharing unpublished data from his earlier work.

FUNDING

This work was partially supported by a National Science Foundation (NSF) Integrated Graduate Education and Research Training award (JCL) and by the Walters Endowed Professorship (JWD). Logistic support was provided by the Barrow Arctic Research Center through NSF-Office of Polar Programs award [0908724] to JWD.

Conflict of interest. None declared.

REFERENCES

Anderson DM. Ice nucleation and the substrate-ice interface. *Nature* 1967;**216**:563–6.

Antón J, Rosselló-Mora R, Rodriguez-Valera F *et al.* Extremely halophilic *Bacteria* in crystallizer ponds from solar salterns. *Appl Environ Microb* 2000;**66**:3052–7.

Barber DG, Ehn JK, Pućko M *et al.* Frost flowers on young Arctic sea ice: The climatic, chemical, and microbial significance of an emerging ice type. *J Geophys Res-Atmos* 2014:593–612.

Boetius A, Anesio AM, Deming JW *et al.* Microbial ecology of the cryosphere: sea ice and glacial habitats. *Nat Rev Microbiol* 2015;**13**:677–90.

Boetius A, Ravenschlag K, Schubert CJ *et al.* A marine microbial consortium apparently mediating anaerobic oxidation of methane. *Nature* 2000;**407**:623–6.

Bowman JS, Deming JW. Elevated bacterial abundance and exopolymers in saline frost flowers and implications for atmospheric chemistry and microbial dispersal. *Geophys Res Lett* 2010;**37**:1–5.

Brigham-Grette J, Hopkins DM. Emergent marine record and paleoclimate of the last interglaciation along the northwest Alaskan coast. *Quat Res* 1995;**43**:159–73.

Brown J. Radiocarbon dating, Barrow, Alaska. *Arctic* 1965;**18**:36–49.

Brown J. Buried soils associated with permafrost. In: Pawluk S (ed.). *Pedology and Quaternary Research*. Edmondton, Alberta: National Research Council of Canada, 1969, 115–27.

Canfield DE, Ngombi-Pemba L, Hammarlund EU *et al.* Oxygen dynamics in the aftermath of the Great Oxidation of Earth's atmosphere. *P Natl Acad Sci USA* 2013;**110**:16736–41.

Colangelo-Lillis J, Wing BA, Whyte LG. Low viral predation pressure in cold hypersaline Arctic sediments and limits on lytic replication. *Environ Microbiol Rep* 2016;**8**:250–60.

Colangelo-Lillis JR, Deming JW. Genomic analysis of cold-active Colwelliaphage 9A and psychrophilic phage-host interactions. *Extremophiles* 2013;**17**:99–114.

Collins RE, Carpenter SD, Deming JW. Spatial heterogeneity and temporal dynamics of particles, bacteria, and pEPS in Arctic winter sea ice. *J Marine Syst* 2008;**74**:902–17.

Collins RE, Deming JW. Abundant dissolved genetic material in Arctic sea ice part II: viral dynamics during autumn freeze-up. *Polar Biol* 2011;**34**:1831–41.

Cox GFN, Weeks WF. Equations for determining the gas and brine volumes in sea-ice samples. *J Glaciol* 1983;**29**:306–16.

Craig H. Isotopic variations in meteoric waters. *Science (80-)* 1961;**133**:1702–3.

Danovaro R, Manini E, Dell'Anno A. Higher abundance of bacteria than of viruses in deep Mediterranean sediments. *Appl Environ Microb* 2002;**68**:1468–72.

Dansgaard W. Stable isotopes in precipitation. *Tellus A* 1964;**16**:436–68.

Dash JG, Rempel AW, Wettlaufer JS. The physics of premelted ice and its geophysical consequences. *Rev Mod Phys* 2006;**78**: 695–741.

Decho AW. Microbial exopolymer secretions in ocean environments: their role(s) in food webs and marine processes. *Oceanogr Mar Biol* 1990;**28**:73–153.

DeMaere MZ, Williams TJ, Allen MA *et al.* High level of intergenera gene exchange shapes the evolution of haloarchaea in an isolated Antarctic lake. *P Natl Acad Sci USA* 2013;**110**: 16939–44.

Deming JW. Sea ice bacteria and viruses. In: Thomas DN, Dieckmann GS (eds). *Sea Ice—An Introduction to Its Physics, Chemistry, Biology and Geology*. 2nd ed. Oxford: Blackwell Publishing Ltd., 2010, 247–82.

Douglas TA, Domine F, Barret M *et al.* Frost flowers growing in the Arctic ocean-atmosphere-sea ice-snow interface: 1. Chemical composition. *J Geophys Res-Atmos* 2012;**117**:1–15.

Dubois M, Gilles KA, Ton JKH *et al.* Colorimetric method for determination of sugars and related substances. *Anal Chem* 1956;**28**:350–6.

Duhaime MB, Deng L, Poulos BT *et al.* Towards quantitative metagenomics of wild viruses and other ultra-low concentration DNA samples: A rigorous assessment and optimization of the linker amplification method. *Environ Microbiol* 2012;**14**:2526–37.

Duran R. Marinobacter. In: Timmis KN (ed.). *Handbook of Hydrocarbon and Lipid Microbiology*. Berlin Heidelberg: Springer-Verlag, 2010, 1726–35.

Edwards KJ, Rogers DR, Wirsen CO *et al.* Isolation and characterization of novel psychrophilic, neutrophilic, Fe-oxidizing, chemolithoautotrophic alpha- and gamma-proteobacteria from the deep sea. *Appl Environ Microb* 2003;**69**: 2906–13.

Ehlmann BL, Mustard JF, Murchie SL *et al.* Subsurface water and clay mineral formation during the early history of Mars. *Nature* 2011;**479**:53–60.

Eicken H, Gradinger R, Kaufman M *et al.* Sea-ice core measurements (SIZONET). *UCAR/NCAR—CISL—ACADIS* 2012, http://dx.doi.org/10.5065/D63X84KG.

Eicken H, Grenfell TC, Perovich DK *et al.* Hydraulic controls of summer Arctic pack ice albedo. *J Geophys Res-Ocean* 2004;**109**:1–13.

Eicken H. Deriving modes and rates of ice growth in the Weddell Sea from microstructural, salinity and stable-isotope data. In: Jeffries MO (ed.). *Antarctic Sea Ice: Physical Processes, Interactions and Variability*. Vol 74. Washington DC, USA: American Geophysical Union, 1998, 89–122.

Engel A, Passow U. Carbon and nitrogen content of transparent exopolymer particles (TEP) in relation to their Alcian Blue adsorption. *Mar Ecol-Prog Ser* 2001;**219**:1–10.

Ewert M. Microbial challenges and solutions to inhabiting the dynamic architecture of saline ice formations. *PhD Thesis* University Washington, Seattle, WA 2013.

Ewert M, Carpenter SD, Colangelo-Lillis J *et al.* Bacterial and extracellular polysaccharide content of brine-wetted snow over Arctic winter first-year sea ice. *J Geophys Res-Ocean* 2013;**118**:726–35.

Ewert M, Deming J. Sea ice microorganisms: Environmental constraints and extracellular responses. *Biology* 2013;**2**:603–28.

Gilichinsky D, Rivkina E, Bakermans C *et al.* Biodiversity of cryopegs in permafrost. *FEMS Microbiol Ecol* 2005;**53**:117–28.

Gilichinsky D, Rivkina E, Shcherbakova V *et al.* Supercooled water brines within permafrost-an unknown ecological niche for microorganisms: a model for astrobiology. *Astrobiology* 2003;**3**:331–41.

Girvan MS, Campbell CD, Killham K *et al.* Bacterial diversity promotes community stability and functional resilience after perturbation. *Environ Microbiol* 2005;**7**:301–13.

Grant WD. Life at low water activity. *Philos T Roy Soc B* 2004;**359**:1249–66.

Guibaud G, Comte S, Bordas F *et al.* Comparison of the complexation potential of extracellular polymeric substances (EPS), extracted from activated sludges and produced by pure bacteria strains, for cadmium, lead and nickel. *Chemosphere* 2005;**59**:629–38.

Henn MR, Sullivan MB, Stange-Thomann N *et al.* Analysis of high-throughput sequencing and annotation strategies for phage genomes. *PLoS One* 2010;**5**:1–12.

Hoffman PF. A neoproterozoic snowball Earth. *Science* 1998;**281**:1342–6.

Kellogg CTE, Deming JW. Comparison of free-living, suspended particle, and aggregate-associated bacterial and archaeal communities in the Laptev Sea. *Aquat Microb Ecol* 2009;**57**: 1–18.

Keys J. Saline discharge at the terminus of the Taylor Glacier. *Antarct J US* 1979;**14**:82–5.

Kochkina GA, Ivanushkina NE, Akimov VN *et al.* Halo- and psychrotolerant *Geomyces* fungi from arctic cryopegs and marine deposits. *Mikrobiologiia* 2007;**76**:39–47.

Krembs C, Eicken H, Deming JW. Exopolymer alteration of physical properties of sea ice and implications for ice habitability and biogeochemistry in a warmer Arctic. *P Natl Acad Sci USA* 2011;**108**:3653–8.

Krembs C, Eicken H, Junge K *et al.* High concentrations of exopolymeric substances in Arctic winter sea ice: implications for the polar ocean carbon cycle and cryoprotection of diatoms. *Deep-Sea Res Pt I* 2002;**49**:2163–81.

Laybourn-Parry J, Marshall WA, Madan NJ. Viral dynamics and patterns of lysogeny in saline Antarctic lakes. *Polar Biol* 2007;**30**:351–8.

Liu S-B, Chen X-L, He H-L *et al*. Structure and ecological roles of a novel exopolysaccharide from the arctic sea ice bacterium *Pseudoalteromonas* sp. strain SM20310. *Appl Environ Microb* 2013;**79**:224–30.

McKay C, Stoker C, Glass B *et al*. The Icebreaker Life Mission to Mars: a search for biomolecular evidence for life. *Astrobiology* 2013;**13**:334–54.

Madan NJ, Marshall WA, Laybourn-Parry J. Virus and microbial loop dynamics over an annual cycle in three contrasting Antarctic lakes. *Freshwater Biol* 2005;**50**:1291–300.

Mancuso Nichols CA, Garon S, Bowman JP *et al*. Production of exopolysaccharides by Antarctic marine bacterial isolates. *J Appl Microbiol* 2004;**96**:1057–66.

Mancuso Nichols CA, Guezennec J, Bowman JP. Bacterial exopolysaccharides from extreme marine environments with special consideration of the Southern Ocean, sea ice, and deep-sea hydrothermal vents: a review. *Mar Biotechnol* 2005;**7**:253–71.

Maranger R, Bird DF, Juniper SK. Viral and bacterial dynamics in Arctic sea ice during the spring algal bloom near Resolute, NWT, Canada. *Mar Ecol-Prog Ser* 1994;**111**:121–8.

Marion GM, Kargel JS. *Cold Aqueous Planetary Geochemistry with FREZCHEM*. Berlin: Springer, 2008.

Marx JG, Carpenter SD, Deming JW. Production of cryoprotectant extracellular polysaccharide substances (EPS) by the marine psychrophilic bacterium *Colwellia psychrerythraea* strain 34H under extreme conditions. *Can J Microbiol* 2009;**55**:63–72.

Maus S, Müller S, Büttner J *et al*. Ion fractionation in young sea ice from Kongsfjorden, Svalbard. *Ann Glaciol* 2011;**52**:301–10.

Meese DA. *The Chemical And Structural Properties Of Sea Ice In The Southern Beaufort Sea*. Hanover, NH, USA: CRREL, 1989, 89–25.

Meyer F, Paarmann D, D'Souza M *et al*. The metagenomics RAST server – a public resource for the automatic phylogenetic and functional analysis of metagenomes. *BMC Bioinformatics* 2008;**9**:386.

Meyer H, Schirrmeister L, Yoshikawa K *et al*. Permafrost evidence for severe winter cooling during the Younger Dryas in northern Alaska. *Geophys Res Lett* 2010;**37**:1–6.

Mikucki JA, Pearson A, Johnston DT *et al*. A contemporary microbially maintained subglacial ferrous 'ocean'. *Science* 2009;**324**:397–400.

Mikucki JA, Priscu JC. Bacterial diversity associated with Blood Falls, a subglacial outflow from the Taylor Glacier, Antarctica. *Appl Environ Microb* 2007;**73**:4029–39.

Millero FJ, Feistel R, Wright DG *et al*. The composition of standard seawater and the definition of the reference-composition salinity scale. *Deep-Sea Res Pt I* 2008;**55**:50–72.

Murray AE, Kenig F, Fritsen CH *et al*. Microbial life at –13°C in the brine of an ice-sealed Antarctic lake. *P Natl Acad Sci USA* 2012;**109**:20626–31.

Murray AG, Jackson GA. Viral dynamics: a model of the effects of size, shape, motion and abundance of single-celled planktonic organisms and other particles. *Mar Ecol-Prog Ser* 1992;**89**:103–16.

Noble RT, Fuhrman JA. Use of SYBR Green I for rapid epifluorescence counts of marine viruses and bacteria. *Aquat Microb Ecol* 1998;**14**:113–8.

Paterson H, Laybourn-Parry J. Antarctic sea ice viral dynamics over an annual cycle. *Polar Biol* 2012;**35**:491–7.

Pecheritsyna SA, Rivkina EM, Akimov VN *et al*. *Desulfovibrio arcticus* sp. nov., a psychrotolerant sulfate-reducing bacterium from a cryopeg. *Int J Syst Evol* **Micr** 2012;**62**:33–7.

Pecheritsyna SA, Shcherbakova VA, Kholodov AL *et al*. Microbiological analysis of cryopegs from the Varandei Peninsula, Barents Sea. *Mikrobiologiia* 2007;**76**:694–701.

Perreault NN, Andersen DT, Pollard WH *et al*. Characterization of the prokaryotic diversity in cold saline perennial springs of the Canadian high arctic. *Appl Environ Microbiol* 2007;**73**:1532–43.

Pollack JB, Kasting JF, Richardson SM *et al*. The case for a wet, warm climate on early Mars. *Icarus* 1987;**71**:203–24.

Rankin LM, Gibson JAE, Franzmann PD *et al*. The chemical stratification and microbial communities of Ace Lake, Antarctica: a review of the characteristics of a marine-derived meromictic lake. *Polarforschung* 1996;**66**:33–52.

Rodriguez-Brito B, Li L, Wegley L *et al*. Viral and microbial community dynamics in four aquatic environments. *ISME J* 2010;**4**:739–51.

Rohwer F, Thurber RV. Viruses manipulate the marine environment. *Nature* 2009;**459**:207–12.

Roux S, Faubladier M, Mahul A *et al*. Metavir: a web server dedicated to virome analysis. *Bioinformatics* 2011;**27**:3074–5.

Santos F, Yarza P, Parro V *et al*. Culture-independent approaches for studying viruses from hypersaline environments. *Appl Environ Microb* 2012;**78**:1635–43.

Shcherbakova V, Chuvilskaya N, Rivkina E *et al*. *Celerinatantimonas yamalensis* sp. nov., a cold-adapted diazotrophic bacterium from a cold permafrost brine. *Int J Syst Evol* **Micr** 2013;**63**:4421–7.

Shcherbakova V, Rivkina E, Laurinavichuis K *et al*. Physiological characteristics of bacteria isolated from water brines within permafrost. *Int J Astrobiol* 2004;**3**:37–43.

Shcherbakova VA, Chuvil'skaia NA, Rivkina EM *et al*. Novel halotolerant bacterium from cryopeg in permafrost: description of *Psychrobacter muriicola* sp. nov. Mikrobiologiia 2009;**78**:98–105.

Shcherbakova VA, Chuvilskaya NA, Rivkina EM *et al*. Novel psychrophilic anaerobic spore-forming bacterium from the overcooled water brine in permafrost: Description *Clostridium algoriphilum* sp. nov. *Extremophiles* 2005;**9**:239–46.

Siegel BZ, McMurty G, Siegel SM *et al*. Life in the calcium chloride environment of Don Juan Pond, Antarctica. *Nature* 1979;**280**:828–9.

Stoderegger K, Herndl GJ. Production and release of bacterial capsular material and its subsequent utilization by marine bacterioplankton. *Limnol Oceanogr* 1998;**43**:877–84.

Thomas DN, Papadimitriou S, Michel C. Biogeochemistry of sea ice. Sea ice—an introduction to its physics, chemistry, biology and geology. In: Thomas DN, Dieckmann GS (eds). 2nd edn. Oxford, UK: Blackwell Publishing Ltd., 2010, 425–67.

Tolstikhin NE, Tolstikhin ON. Groundwater and surface water in the permafrost region. In: Melnikov PI, Tolstikhin ON (eds). *General Permafrost Studies*. Novosibirsk: USSR Academy of Sciences, 1974, 1974.

Underwood GJC, Aslam SN, Michel C *et al*. Broad-scale predictability of carbohydrates and exopolymers in Antarctic and Arctic sea ice. *P Natl Acad Sci USA* 2013;**110**:15734–9.

Wais AC, Daniels LL. Populations of bacteriophage infecting *Halobacterium* in a transient brine pool. *FEMS Microbiol Lett* 1985;**31**:323–6.

Ward BB, Martino DP, Diaz MC *et al*. Analysis of ammonia-oxidizing bacteria from hypersaline Mono Lake, California, on the basis of 16S rRNA sequences. *Appl Environ Microb* 2000;**66**:2873–81.

Wells LE, Deming JW. Characterization of a cold-active bacteriophage on two psychrophilic marine hosts. *Aquat Microb Ecol* 2006a;**45**:15–29.

Wells LE, Deming JW. Effects of temperature, salinity and clay particles on inactivation and decay of cold-active marine bacteriophage 9A. *Aquat Microb Ecol* 2006b;**45**:31–9.

Wells LE, Deming JW. Modelled and measured dynamics of viruses in Arctic winter sea-ice brines. *Environ Microbiol* 2006c;**8**:1115–21.

van Everdingen RO. Geocryological terminology. *Can J Earth Sci* 1976;**13**:862–7.

van der Wielen PWJJ, Bolhuis H, Borin S *et al.* The enigma of prokaryotic life in deep hypersaline anoxic basins. *Science* 2005;**307**:121–3.

Williams PJB. Analysis: Organic matter. In: Head PC (ed.). *Practical Estuarine Chemistry: A Handbook*. Cambridge: Cambridge University Press, 1985, 160–200.

Wommack KE, Colwell RR. Virioplankton: viruses in aquatic ecosystems. *Microbiol Mol Biol R* 2000;**64**:69–114.

Wrede C, Kokoschka S, Dreier A *et al.* Deposition of biogenic iron minerals in a methane oxidizing microbial mat. *Archaea* 2013;**2013**:102972, DOI: 10.1155/2013/102972.

Yau S, Lauro FM, DeMaere MZ *et al.* Virophage control of antarctic algal host-virus dynamics. *P Natl Acad Sci USA* 2011;**108**:6163–8.

Yoshikawa K, Romanovsky V, Duxbury N *et al.* The use of geophysical methods to discriminate between brine layers and freshwater taliks in permafrost regions. *J Glaciol Geocryol* 2004;**26**:301–9.